

Quasi-particle scattering and protected nature of topological states in a parent topological insulator Bi_2Se_3

S. R. Park¹, W. S. Jung¹, Chul Kim¹, D. J. Song¹, C. Kim^{1,*}, S. Kimura², K. D. Lee³ and N. Hur³

¹*Institute of Physics and Applied Physics, Yonsei University, Seoul, Korea*

²*UVSOR Facility, Institute for Molecular Science and The Graduate University for Advanced Studies, Okazaki 444-8585, JAPAN and*

³*Department of Physics, Inha University, Incheon 402-751, Korea*

(Dated: November 5, 2018)

We report on angle resolved photoemission spectroscopic studies on a parent topological insulator (TI), Bi_2Se_3 . The line width of the spectral function (inverse of the quasi-particle lifetime) of the topological metallic (TM) states shows an anomalous behavior. This behavior can be reasonably accounted for by assuming decay of the quasi-particles predominantly into bulk electronic states through electron-electron interaction and defect scattering. Studies on aged surfaces reveal that topological metallic states are very much unaffected by the potentials created by adsorbed atoms or molecules on the surface, indicating that topological states could be indeed protected against weak perturbations.

PACS numbers: 81.05.Uw, 63.20.kk, 73.20.At, 79.60.-i

TIs are materials with bulk gaps due to spin-orbit coupling. TIs are classified into ‘weak TI’ and ‘strong TI’ according to Z_2 topological invariants.^{2,3} Strong TIs have odd number of TM Dirac cones on the surface which is robust (protected) against disorder or impurities.

TM states realized on the surface of a strong TI is important and could be useful.^{4,5} The properties of the TM are also set by the topological nature of the TI. The essential properties of TMs can be summarized as follows. First, electron spins in TM are locked into the momenta, forming spin chiral states⁶. Such spin chiral states are also well known in the field of surface science in terms of Rashba effects in surface states (for example, Sb (111)⁷, Bi(111)⁸ and Au (111)⁹ surfaces states). Second, back scattering is suppressed due to the spin chirality,¹⁰ meaning relatively long quasi-particle life time. Third, metallic bands are protected against perturbations to the first order due to the topological nature. This point has yet to be experimentally observed.

Experimental verification of the novel properties of TM is not only important in the fundamental aspect but also necessary for use of these materials for future applications. Due to the surface nature of the TM states, most of the experimental data thus far came from angle resolved photoemission (ARPES)^{6,11–13} and to a less degree from scanning tunnelling microscopy (STM).¹⁰ By using ARPES, it was shown that there exist odd number of bands crossing the Fermi level in this class of materials.^{11,12} Moreover, spin resolved photoemission results show that the electron spins are indeed locked into the momentum and form spin chiral states.⁶ As for STM studies, a recent study shows suppression of back scattering, consistent with spin chiral states.¹⁰

Studies mentioned above are about existence and spin chiral states of TM and experimental verification of whether topological states are in general protected or not has not been discussed. Protected topological states should manifest themselves with long quasi-particle life

time. In that regards, ARPES is an important tool because long quasi-particle life time should result in a sharp ARPES line-shape. In spite of the intensive recent efforts on TM electronic structure studies, photoemission line-shape issue has not been addressed. This point, however, is important because recent discussions on the use of TIs for spintronic applications require very low scattering rate to properly convey the spin information.

To address the quasi-particle lifetime issue, high resolution ARPES data on various TIs have to be obtained. We begin the effort with studies on a parent TI Bi_2Se_3 . The goal of this work is to analyze the high quality ARPES spectral function in terms of various scattering channels to see the mechanisms behind the quasi-particle scattering. In that analysis, the bulk states play an important role in quasi-particle dynamics in the TM band: Electrons in TM are strongly scattered to the bulk electronic states by coupling to phonons, impurity or defect created potentials and other electrons. In addition, we find the TM states protected against adsorbate induced disorder potentials.

Single crystals were grown by a self flux technique, following the previously reported recipe.¹⁶ ARPES measurements were performed at the beam line 7U of UVSOR-II¹⁷. Various photon energies between 8 and 21 eV were used. The total energy resolution was set to be 10 meV at 8 eV, and the angular resolution was 0.1 degree. Samples were cleaved *in situ* and the chamber pressure was about 2×10^{-10} torr. The measurement temperature was kept at 15 K.

ARPES data from Bi_2Se_3 (111) are plotted in Figure 1. Panel (a) shows data from freshly cleaved surface with 8 eV photon. Relatively sharp and strongly dispersive electron pocket is observed. This is the TM band having a helical spin structure.⁶ As indicated by white arrow in the panel, position of the TM band at the Γ point (Dirac point) is around 0.33 eV. One can also see broad weak feature near E_F at the Γ point which originates from the

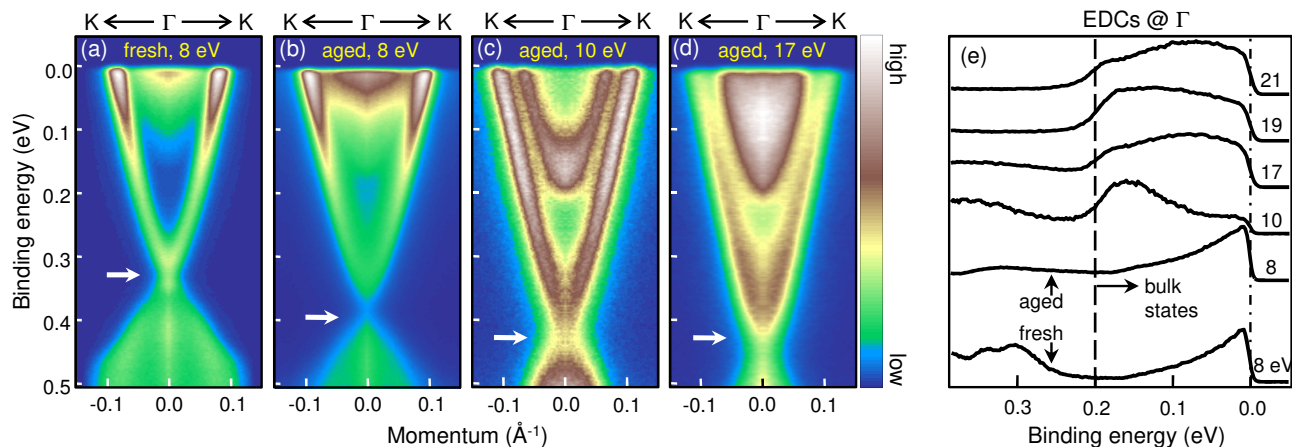


FIG. 1. ARPES data taken with (a) 8 eV, (b) 8 eV, (b) 10 eV and (c) 17 eV photon energies along the Γ to K points. The data in (a) were taken on a freshly cleaved surfaces while data in (b)-(d) were taken on aged (4 day old) surfaces. (d) EDCs at the Γ point taken with various photon energies

bulk states.¹¹

Panels (b) shows ARPES data taken with the same photon energy but 4 days after cleaving (aged surface). It is remarkable to note that the TM band feature remains intact and looks almost the same as that from a freshly cleaved surface. One difference is that the Dirac point is now located at around 0.43 eV, about 0.1 eV higher than the original position. This shift of the Dirac point is attributed to charge transfer from physisorbed atoms or molecules. While a similar surface doping effect in Bi_2Te_3 has already been discussed,¹³⁻¹⁵ no such effect has been reported in $\text{Bi}_2\text{Se}_3(111)$. The difference in the bulk states other than the uniform shift is due to the k_z -selection rule which will be discussed below.

Figure 1c and 1d plot the data from aged surface taken with 10 and 17 eV. Compared to 8 eV data, they have almost the same TM features while bulk bands look quite different. To see the photon energy dependence more clearly, we plot in figure 1(d) energy distribution curves (EDCs) at the Γ point from fresh and aged surfaces taken with various photon energies between 8 eV and 21 eV. The bulk state feature in the EDC taken with 8 eV photon is relatively sharp. This feature becomes broader as photon energy increases. This can be explained by the decreasing photoelectron life time with increasing photon energy, resulting in inclusion of a broader range of k_z .¹⁸ This, in combination with the fact that probed k_z varies with the photon energy, results in clear observation of the bulk conduction band bottom (BCBB) edge at about 0.2 eV in the EDCs taken with 17, 19 and 21 eV photons as indicated by the dashed line in Figure 1(d) while 8 eV EDC does not display a clear BCBB edge. In addition, 10 eV is the right photon energy to observe the BCBB as can be seen in Figure 1(b) and 1(d). Considering the fact that there is 0.1 eV shift in the band position between fresh and aged surfaces, we can determine that BCBB of the fresh surface is at about 0.1 eV.

We now wish to analyze the self energy of the TM

states. Before we proceed to analyzing the actual data, however, we need to touch upon various scattering channels. In estimating the self energy, we note that scattering between TM electrons should be small due to the limited number of states (compared to the bulk states) and helical spin structure.¹⁰ Therefore, the dominant mechanism for TM electron (or hole) decay is through transition to bulk states. Figure 2(a) shows possible scattering channels between a hole in the TM states and a bulk electron. A hole in the TM state may decay into a bulk electronic state with the total energy and momentum conserved through electron-hole (e-h) pair creation, phonon emission or absorption, and impurity created potential as illustrated in Figure 2(a). A rough estimate of the imaginary part of the TM electron self-energy (or $1/\tau$) can be made by calculating the available phase space volume. We assume that phonons between 0 and 0.03 eV equally contribute to scattering and also that the bulk density of states is proportional to $(E - E_{BB})^{1/2}$ where E_{BB} is the BCBB energy. A schematic of the result at 0 K is shown in Figure 2(b). While $\text{Im}\Sigma$ in the Fermi liquid theory¹⁹ increases proportional to ω^2 , $\text{Im}\Sigma$ due to e-h pair creation in Bi_2Se_3 increases at low binding energy side and saturates slightly after E_{BB} . On the other hand, phonons and impurities provide major scattering channels for the states with binding energies lower than E_{BB} . These channels however do not contribute for the states with binding energies higher than E_{BB} .

ARPES spectral function $A(k, \omega)$ is proportional to the imaginary part of the Greens function

$$\text{Im}G(k, \omega) = \frac{\text{Im}\Sigma(k, \omega)}{(\omega - \varepsilon_k - \text{Re}\Sigma(k, \omega))^2 + \text{Im}\Sigma(k, \omega)^2} \quad (1)$$

If the self energy $\Sigma(k, \omega)$ is slowly varying with ω , EDCs are Lorentzians and the half width at half maximum (HWHM) of each EDC gives $\text{Im}\Sigma$. Extracted EDC peak width has been used to study the electron dynamics in $\text{Mo}(111)$ surfaces states and cuprates.²⁰⁻²² Fitting an

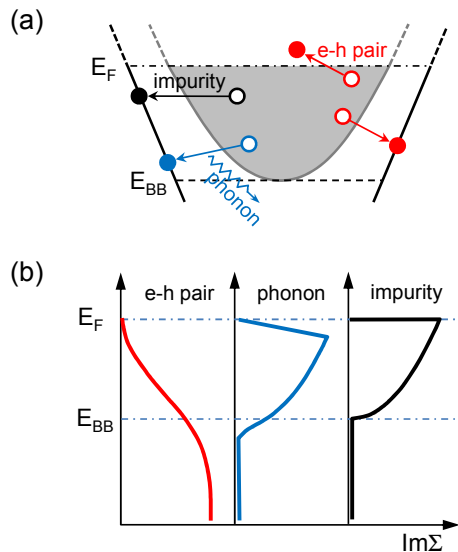


FIG. 2. (a) Schematic of various scattering channels for a photo-hole in the TM band. Only the transition to the bulk states are considered. (b) Corresponding $\text{Im}\Sigma$ for various channels.

EDC with a Lorentzian function however is often difficult in correlated materials due to, for example, the incoherent spectral weight. Instead, a commonly used method is to obtain $\text{Im}\Sigma$ by multiplying HWHMs of momentum distribution curves (MDCs) by the band velocity,^{23,24} which we also use in analyzing the data. Another note is that it helps to isolate the TM contribution of the spectral function. In the case of Bi_2Se_3 (111), bulk bands are located close to the TM band, making it difficult to extract the TM spectral weight from ARPES data precisely. However, we note that the bulk state spectral function taken with 8 eV photon is much more suppressed than other data sets as shown in Figure 1 (a)-(c). This is, as discussed above, k_z -selection rule suppresses photoemission from the bulk states at this photon energy. This provides us an opportunity to extract the TM spectral function and do self energy analysis more reliably. We thus analyze and present self energy analysis on 8 eV data.

Figure 3(a) plots $\text{Im}\Sigma$ from fresh and aged surfaces. $\text{Im}\Sigma$ initially increases but starts to decrease at around 0.10 eV and 0.17 eV binding energies for fresh and aged surfaces, respectively. In addition, the fresh surface data hints flattening of $\text{Im}\Sigma$ curve from 0.25 eV binding energy. These behaviors contrast with ordinary metallic cases where $\text{Im}\Sigma$ monotonically increases due to electron-electron scattering.^{19,20,22-24} The decrease in $\text{Im}\Sigma$ reminds us of the drop in $\text{Im}\Sigma$ from phonon and impurity channels at E_{BB} . Thus we can attribute the $\text{Im}\Sigma$ behavior to the fact that TM electrons are dominantly scattered to bulk electronic states which exist only below E_{BB} .

We analyze the experimental $\text{Im}\Sigma$ of the 8 eV data from fresh surfaces based on the interpretation illustrated

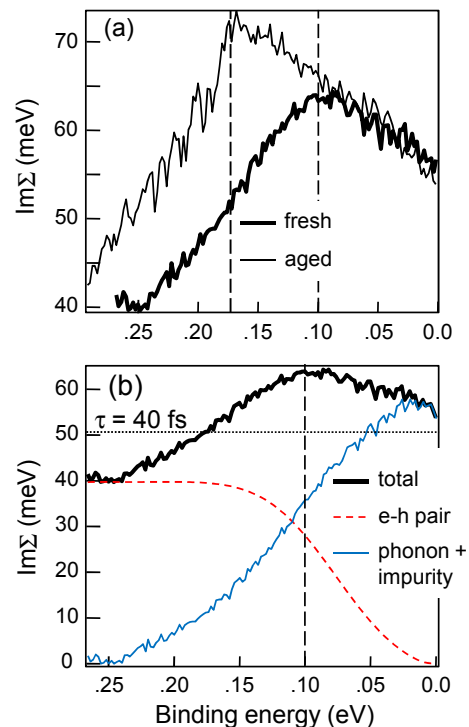


FIG. 3. (a) TM band $\text{Im}\Sigma$ from fresh and aged surfaces of Bi_2Se_3 (111) taken with 8 eV photons. (b) Analysis of $\text{Im}\Sigma$ from fresh surface in terms of e-h pair creation, and phonon plus impurity channels.

in Figure 2. The results are plotted in Figure 3(b). It is seen from the result that, while $\text{Im}\Sigma$ at high energy side mainly come from electron-electron interaction (electron-hole pair creation) channel, impurity and phonon channels dominate the low energy dynamics which controls the transport properties. As contributions from both impurity and phonon channels are approximately proportional to the bulk density of states, it is difficult to distinguish them. However, we believe that the low energy part of $\text{Im}\Sigma$ mainly comes from the defect scattering because characteristic phonon kink in $\text{Im}\Sigma$ illustrated in Figure 2(b) was not observed. This is not unreasonable considering the fact that these materials tend to be non-stoichiometric. This will be the main obstacle to overcome if dissipationless spin current on TIs were to be realized. The life time (τ) and mean free path (l_m) of the electrons near E_F are roughly $\tau=40$ fs and $l_m = \tau \times v_g = 0.02\mu\text{m}$, respectively.

As discussed above, decay of quasi-particles in TM states appear to mainly come from scattering to the bulk states, not to other TM states. Indeed, there are indications in other ARPES data that the intrinsic life time of quasi-particles in TM bands is fairly long. For example, Bi_2Te_3 shows a relatively sharp ARPES lineshape.¹³ Even though not an insulator, $\text{Sb}(111)$ also has TM states with very sharp ARPES peaks²⁵. For the low energy electron dynamics, we showed that defect scattering plays the main role. It is therefore important to make stoichio-

metric Bi_2Se_3 not only to make insulating bulk states but also to reduce the scattering between TM and bulk states.

Finally, we discuss if the TM states are protected. We observe that the Fermi surface volume of the TM band from aged surfaces increased about 2.3% compared to that of the fresh surfaces, which means that at least 0.023 electrons per surface unit cell are transferred presumably from adsorbed atoms or molecules on the sample surface. Assuming that each atom or molecule donates 1 electron and that all the donated electrons are localized at the surface states, there are $6 \times 10^{13}/\text{cm}^2$ adsorbate atoms/molecules which translates into $\approx 13\text{\AA}$ inter-adsorbate distance. Considering the fact that bulk states also receive electrons, the inter-adsorbate distance should be shorter. Since the adsorbates should induce disorder potential near the surface, additional scattering channels between surface electrons in ordinary cases. Therefore, we expect an increase in $\text{Im}\Sigma$ near E_F . However, we do not observe such increase in the data in Figure 3(a). Please note that the mean free path estimated from the life time in Figure 3(b) is about 200 \AA , much longer than the estimated inter-adsorbate distance.

There can be different reasons why the scattering rate

did not increase. Interesting case would be from the protected nature of the TM states. The estimated number of adsorbate atoms or molecules on the surface may be enough to increase the scattering rate substantially. However, the scattering rate may have not increased because the TM states are topologically protected from weak disorder from the potential induced by adsorbates. If it is indeed the case, this would be the first experimental evidence from ARPES for the protected nature of TM states, to our best knowledge. However, one has to be careful not to make a foregone conclusion because the induced potential can vary depending on the adsorbates. For example, relatively small amount of H atoms on graphene destroys the metallic states while K atoms have almost no effect except electron doping.²⁶ In order to resolve this issue, we propose a controlled ARPES experiments in combination with first principles electronic structure calculations.

Authors acknowledge fruitful discussions with J.H.Han. This work is supported by NRF (20090080739) and by KOSEF (F01-2007-000-10117-0). SRP is supported by the 2009 Yonsei University Research Fund. NH acknowledges support from Korea Research Foundation through KRF-2008-331-C00093

* Electronic address: cykim@phya.yonsei.ac.kr

² Liang Fu, C. L. Kane and E. J. Mele, Phys. Rev. Lett. **98**, 106803 (2007).

³ Liang Fu and C. L. Kane, Phys. Rev. B **76**, 045302 (2007).

⁴ Charles Day, Physics Today, January 2008, 19-23 (2008).

⁵ Enrico Ramirez-Ruiz and William Lee, Nature **460**, 1090-1091 (2009).

⁶ D. Hsieh, Y. Xia, D. Qian, L. Wray, J. H. Dil, F. Meier, J. Osterwalder, L. Patthey, J. G. Checkelsky, N. P. Ong, A. V. Fedorov, H. Lin, A. Bansil, D. Grauer, Y. S. Hor, R. J. Cava and M. Z. Hasan, Nature **460**, 1101-1105 (2009).

⁷ K. Sugawara, T. Sato, S. Souma, T. Takahashi, M. Arai and T. Sasaki, Phys. Rev. Lett. **96**, 046411 (2006).

⁸ Yu. M. Koroteev, G. Bihlmayer, J. E. Gayone, E.V. Chulkov, S. Blügel, P.M. Echenique and Ph. Hofmann, Phys. Rev. Lett. **93**, 046403 (2004).

⁹ F. Reinert, G. Nicolay, S. Schmidt, D. Ehm and S. Hüfner, Phys. Rev. B **63**, 115415 (2001).

¹⁰ Pedram Roushan, Jungpil Seo, Colin V. Parker, Y. S. Hor, D. Hsieh, Dong Qian, Anthony Richardella, M. Z. Hasan, R. J. Cava and Ali Yazdani, Nature **460**, 1106-1109 (2009).

¹¹ Y. Xia, D. Qian, L. Wray, A. Pal, H. Lin, A. Bansil, D. Grauer, Y. S. Hor, R. J. Cava and M. Z. Hasan, Nature Physics **5**, 398-402 (2009).

¹² D. Hsieh, D. Qian, L. Wray, Y. Xia, Y. S. Hor, R. J. Cava and M. Z. Hasan, Nature **452**, 970-974 (2008).

¹³ Y. L. Chen, J. G. Analytis, J.-H. Chu, Z. K. Liu, S.-K. Mo, X. L. Qi, H. J. Zhang, D. H. Lu, Z. Dai, Z. Fang, S. C. Zhang, I. R. Fisher, Z. Hussain and Z.-X. Shen, Science **325**, 178-181 (2009).

¹⁴ H.-J. Noh, H. Koh, S.-J. Oh, J.-H. Park, H.-D. Kim, J. D. Rameau, T. Valla, T. E. Kidd, P. D. Johnson, Y. Hu and Q. Li, Europhys. Lett. **81**, 57006 (2008).

¹⁵ D. Hsieh, Y. Xia, D. Qian, L. Wray, F. Meier, J. H. Dil, J. Osterwalder, L. Patthey, A. V. Fedorov, H. Lin, A. Bansil, D. Grauer, Y. S. Hor, R. J. Cava and M. Z. Hasan, Phys. Rev. Lett. **103**, 146401 (2009).

¹⁶ Y. S. Hor, A. Richardella, P. Roushan, Y. Xia, J. G. Checkelsky, A. Yazdani, M. Z. Hasan, N. P. Ong, R. J. Cava, Phys. Rev. B **79**, 195208 (2009).

¹⁷ S. Kimura, T. Ito, E. Nakamura, M. Hosaka, M. Katoh, AIP Conf. Proc. **879**, 527 (2007).

¹⁸ N. V. Smith, P. Thiry and Y. Petroff, Phys. Rev. B **47**, 15476-15481 (1993).

¹⁹ R. Claessen, R. O. Anderson, J. W. Allen, C. G. Olson, C. Janowitz, W. P. Ellis, S. Harm, M. Kalning, R. Manzyk and M. Skibowski, Phys. Rev. Lett. **69**, 808-811 (1992).

²⁰ T. Valla, A. V. Fedorov, P. D. Johnson and S. L. Hulbert, Phys. Rev. Lett. **83**, 2085-2088 (1999).

²¹ Chul Kim, S. R. Park, C. S. Leem, D. J. Song, H. U. Jin, H.-D. Kim, F. Ronning and C. Kim, Phys. Rev. B **76**, 104505 (2007).

²² Seung Ryoung Park, D. J. Song, C. S. Leem, Chul Kim, C. Kim, B. J. Kim and H. Eisaki, Phys. Rev. Lett. **101**, 117006 (2008).

²³ P. V. Bogdanov, A. Lanzara, S. A. Kellar, X. J. Zhou, E. D. Lu, W. J. Zheng, G. Gu, J.-I. Shimoyama, K. Kishio, H. Ikeda, R. Yoshizaki, Z. Hussain and Z. X. Shen, Phys. Rev. Lett. **85**, 2581-2584 (2000).

²⁴ X. J. Zhou, Junren Shi, T. Yoshida, T. Cuk, W. L. Yang, V. Brouet, J. Nakamura, N. Mannella, Seiki Komiya, Yoichi Ando, F. Zhou, W. X. Ti, J. W. Xiong, Z. X. Zhao, T. Sasagawa, T. Kakeshita, H. Eisaki, S. Uchida, A. Fujimori, Zhenyu Zhang, E. W. Plummer, R. B. Laughlin, Z. Hussain and Z. X. Shen, Phys. Rev. Lett. **95**, 117001 (2005).

- ²⁵ Kenjiro K. Gomes, Wonhee Ko, Warren Mar, Yulin Chen, Zhi-Xun Shen, Hari C. Manoharan, arXiv:cond-mat/0909.0921.
- ²⁶ Aaron Bostwick, Jessica L. McChesney, Konstantin V.

Emtsev, Thomas Seyller, Karsten Horn, Stephen D. Kevan, and Eli Rotenberg, *Phy. Rev. Lett.* **103**, 056404 (2009).